Crystallization Behavior of A Novel Poly(aryl ether ketone): PEDEKmK

TIANXI LIU,[1] ZHISHEN MO,[1] SHANGER WANG,[1] HONGFANG ZHANG,[1] JUNZUO WANG,[2] HUI NA,[2] ZHONGWEN WU[2]

[1] Changchun Institute of Applied Chemistry, Academia Sinica, Changchun 130022, China

[2] Chemistry Department, Jilin University, Changchun 130023, China

Received 31 May 1996; accepted 20 September 1996

ABSTRACT: Isothermal melt and cold crystallization kinetics of PEDEKmK linked by *meta*-phenyl and biphenyl were investigated by differential scanning calorimetry in two temperature regions. Avrami analysis is used to describe the primary stages of the melt and cold crystallization, with exponent $n = 2$ and $n = 4$, respectively. The activation energies are -118 kJ/mol and 510 kJ/mol for crystallization from the melt and the glassy states, respectively. The equilibrium melting point T_m^0 is estimated to be 309°C by using the Hoffman–Weeks approach, which compares favorably with determination from the Thomson–Gibbs method. The lateral and end surface free energies derived from the Lauritzen–Hoffman spherulitic growth rate equation are $\sigma = 8.45$ erg/cm^2 and $\sigma_e = 45.17$ erg/cm^2, respectively. The work of chain folding q is determined as 3.06 kcal/mol. These observed crystallization characteristics of PEDEKmK are compared with those of the other members of poly(aryl ether ketone) family. © 1997 John Wiley & Sons, Inc. J Appl Polym Sci **64:** 1451–1461, 1997

Key words: PEDEKmK; isothermal melt and cold crystallization kinetics; activation energy; work of chain folding

INTRODUCTION

Semicrystalline polymers, poly(aryl ether ketone)s (PAEKs) such as PEK, PEEK, and PEEKK have been used as high-performance engineering plastics in recent decades. The phenyl rings in PAEKs mentioned above are all *para*-linked, giving rise to a high melting temperature (T_m) which is too high for convenient processing. Recently, other reported variants also contain *meta*-phenyl and biphenyl units in the polymer backbone so as to modify the T_m without adversely reducing the glass transition temperature (T_g).[1–3]

This paper is mainly concerned with that particular variant of PAEKs labeled PEDEKmK, which comprises both biphenyl and *meta*-phenyl units regularly spaced along the chain:

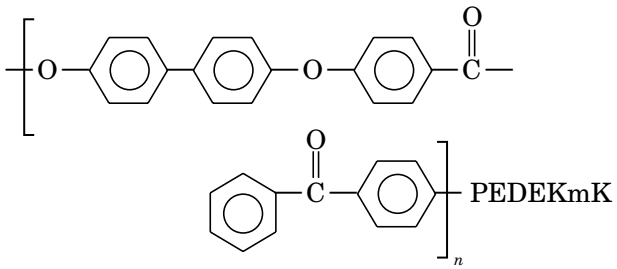

The T_g (160°C) of PEDEKmK is significantly higher than that of PEEK (144°C), but its T_m

Correspondence to: Z. Mo.

Contract grant sponsors: Key Projects of the National Natural Science Foundation of China and National Key Projects for Fundamental Research "Macromolecular Condensed State," The State Science and Technology Commission of China.

© 1997 John Wiley & Sons, Inc. CCC 0021-8995/97/081451-11

(303°C) is lower than that of PEEK (335°C). The Kelvin ratio (T_g/T_m = 0.75) of PEDEKmK compares favorably with that of PEEK (0.69), which is desirable for the higher application temperature combined with lower melting and processing temperatures. The preparation of PEDEKmK and a description of its unusual crystallization and melting behavior have been reported elsewhere (where labeled PK99).[4,5]

In our previous work, the morphology of PEDEKmK was investigated by polarizing optical microscopy, transmission electron microscopy (TEM), differential scanning calorimetry (DSC), small angle X-ray scattering (SAXS), and electron diffraction (ED).[6] A distinct change in lamellar thickness and orientation and spherulitic morphology was observed due to the crystal melting and recrystallization. However, the crystal packing mode was found to be identical before and after recrystallization. Recently, we reported the crystal structure and polymorphism induced by uniaxial drawing of PEDEKmK.[7] Based on TEM, ED, wide angle X-ray diffraction, and DSC techniques, it had been found that the crystal structure of isotropic crystalline PEDEKmK obtained under different crystallization conditions (melt-, cold-, solvent-induced crystallization; melting-recrystallization; and crystallization from solution) keeps the same mode of packing, i.e., two-chain orthorhombic unit cell with dimensions of a = 0.784 nm, b = 0.600 nm, and c = 4.745 nm (form I). A second crystal modification (form II) can be induced by uniaxial drawing above the T_g, which always coexists with form I constituent. This form also possesses an orthorhombic unit cell but with different dimensions of a = 0.470 nm, b = 1.054 nm, and c = 5.064 nm.

The present work reports the isothermal melt and cold crystallization kinetics of PEDEKmK studied by DSC. The observed results of the polymer are compared with those of the other members of its family such as PEEK and PEEKK with different linkages.

EXPERIMENTAL

Materials and Preparation

PEDEKmK was prepared by polycondensation of 1,3-bis(4-fluorobenzoyl)benzene and 4,4′-biphenol in our laboratory. The inherent viscosity of the polymer used is 0.83 dL/g (measured at 25°C on a 0.1% solution of the polymer in 98% sulfuric acid). The number average molecular weight of the sample is 10,000. The transparent amorphous PEDEKmK film was obtained by quickly quenching the hot-press sheets in liquid nitrogen from the polymer melt.

Differential Scanning Calorimetry

Isothermal crystallization kinetics were carried out using a Perkin–Elmer DSC-7 differential scanning calorimeter calibrated with indium and zinc standards. Isothermal crystallization kinetics were performed *in situ* through two kinds of experiments.

1. Isothermal melt crystallization. The samples were heated in DSC quickly (at 80°C/min) to 350°C, held there for 10 min to eliminate residual crystals, then cooled (at −80°C/min) to the designated crystallization temperatures (T_c) which were five different temperatures in the range of 260 to 276°C. The exothermal curves of heat flow as a function of time were recorded and investigated.
2. Isothermal cold crystallization. The amorphous glassy samples were heated (at 80°C/min) to the reset crystallization temperatures (T_c') ranged from 245 to 250°C. The exothermal curves were also recorded and analysed.

All DSC were performed under a nitrogen purge. Sample weights were between 4 and 6 mg.

Small-Angle X-ray Scattering

The SAXS data at room temperature were obtained with a Philips PW-1700 X-ray diffractometer equipped with a Kratky small angle X-ray camera, a step-scanning device, and a scintillation counter. The distance between sample and detector was 20 cm. All measurements were performed with a Cu–Kα radiation source operating at 45 kV and 40 mA. Monochromatization was achieved by using a graphite crystal. The scattering intensities were corrected for absorption, background, and incident X-ray intensity fluctuations of the samples. Desmeared scattering intensities were obtained by using a procedure developed by Glatter.[8]

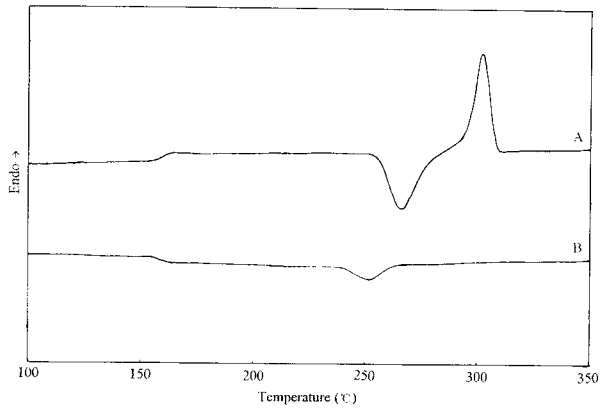

Figure 1 Thermal analysis of PEDEKmK: (A) heating from the amorphous glassy state; (B) cooling from the molten state. (Scanning rate is 20°C/min.)

RESULTS AND DISCUSSION

Isothermal Crystallization Kinetics from Avrami Analysis

The cyclic diagram of thermal analysis for PEDEKmK was recorded by heating the amorphous film from 100°C to 350°C at 10°C/min; holding there for 10 min in order to remove all residues of crystallinity; and then cooling down to 100°C again at 10°C/min (Fig. 1). On heating the amorphous specimen through the glass transition (T_g = 160°C), it exhibited a well-defined crystallization exotherm ($T_{c,h}$ = 265°C) in the region of 248 to 285°C, which was closely followed by a final melting endotherm (T_m = 303°C). While cooling from the melt, a cold-crystallization exotherm ($T_{c,c}$ = 251°C) was in the region of 230 to 270°C. DSC was also used to study the isothermal crystallization by cooling the melt rapidly to the T_c (melt crystallization) and by heating the quenched amorphous glass rapidly to the T_c' (cold-crystallization). Heat-flow curves were recorded as a function of time (Fig. 2). For melt crystallization, as the T_c increased, the crystallization exotherms shifted to higher temperatures and became broad (A). But for cold crystallization, with increasing the T_c', the crystallization exotherms moved to lower temperatures (B). It implies that the rate of melt crystallization increases with decreased T_c, but the rate of cold crystallization increases as the T_c' increases.

Avrami equation[9,10], which assumes that the relative degree of crystallinity develops with time t, was used to analyze the isothermal crystallization process of PEDEKmK. The well-known double logarithmic plot of $\log[-\ln(1 - Xt)]$ versus $\log(t)$ is shown in Figure 3. Each curve shows an initial linear portion, subsequently tending to level off. This deviation was considered to be due to the secondary crystallization which was caused by the spherulite impingement in the later stage. Such leveling off has been also found by Cebe and Hong[11] and Lee and Porter[12] for PEEK. The linear portions are almost parallel to each other, shifting to longer time with increasing the T_c for melt crystallization [Fig. 3(A)]; yet, for cold crystallization [Fig. 3(B)], shifting to longer time with decreasing the T_c'. The Avrami parameters n and k for both melt and cold crystallization, determined from the initial linear portion in Figure 3, are listed in Table I. The average values of Avrami exponents are $n = 2$ and $n = 4$ up to about 80% completion of the melt and cold crystallization processes, respectively. The value of the former exponent suggests that the primary crystallization stage for melt crystallization might correspond to a two-dimensional, circular, diffusion-con-

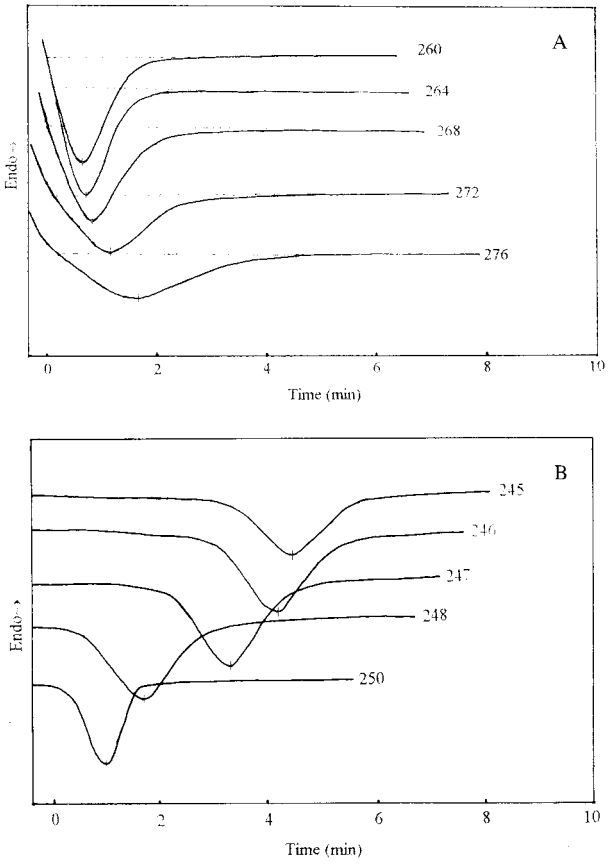

Figure 2 Heat flow versus time during isothermal crystallization of PEDEKmK at the indicated temperatures. (A) melt crystallization; (B) cold crystallization. (Peaks of the curves are indicated by short bars.)

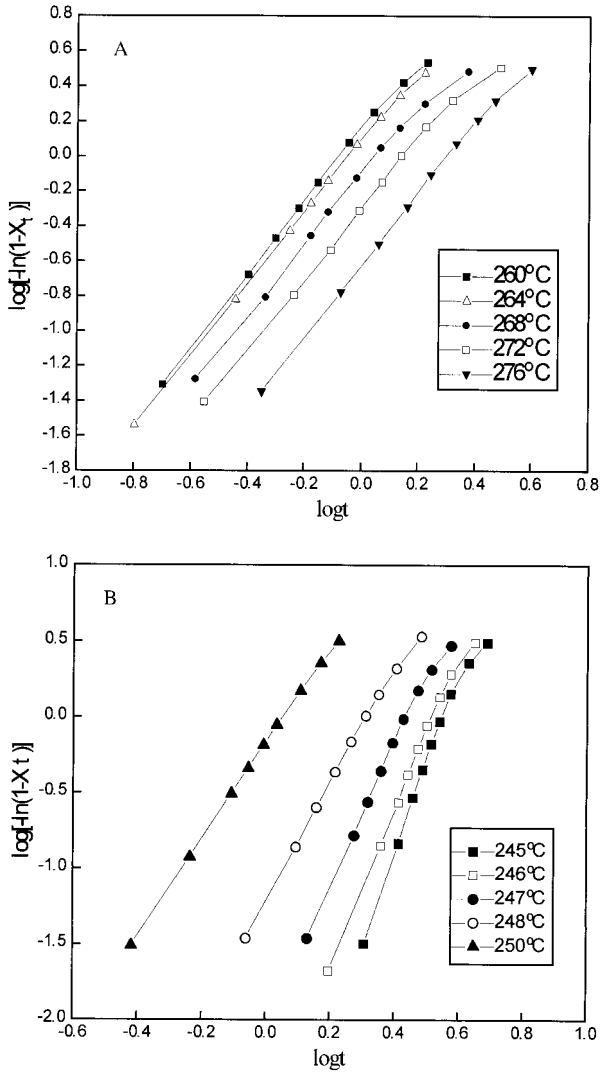

Figure 3 Plots of $\log[-\ln(1 - Xt)]$ versus $\log(t)$ (min) for isothermal crystallization at the indicated temperatures. (A) melt crystallization; (B) cold crystallization.

trolled growth with thermal nucleation.[13] For cold crystallization, $n = 4$, it implies that in the initial crystallization stage, the crystal growing body is three-dimensional and spherical with a thermal nucleation process, in which the nuclei are created sporadically in time and space; the exponent is expected to be 4.[12–13] The values of k decrease with increasing the T_c but increase with increasing the T'_c. Thus the primary crystallization rate parameters k for melt and cold crystallization exhibit very different temperature dependencies characteristic of nucleation-controlled and thermally activated crystallization associated with the proximity of the T_m and the T_g, respectively.

The crystallization half-time is defined as the time at which the extent of crystallization is 50% complete and is determined from the measured kinetic parameters; that is,

$$t_{1/2} = \left(\frac{\ln 2}{k}\right)^{1/n} \tag{1}$$

Usually, the rate of crystallization G is described as the reciprocal of $t_{1/2}$, that is to say, $G = \tau_{1/2} = (t_{1/2})^{-1}$. The values of $t_{1/2}$ and $\tau_{1/2}$ presented in Table I indicate that the rate of melt crystallization is larger than that of cold crystallization, which will be discussed later. Data of the time necessary for maximum crystallization to occur, $t_{\max}$, is shown on the heat-flow curves in Figure 2 by short bars. Since this time corresponds to the point where $dQ/dt = 0$, $Q(t)$ being the heat-flow rate, we can use the Avrami equation to write $t'_{\max}$ in terms of n and k, obtaining

$$t'_{\max} = \left(\frac{(n-1)}{nk}\right)^{1/n} \tag{2}$$

The calculated values of $t'_{\max}$ are listed in Table I, which are quite consistent with the observed ones of $t_{\max}$ determined by calorimetry. This also indicates that the Avrami analysis can be satisfactorily employed to describe the primary stage of isothermal crystallization.

More informative data on the overall crystallization behavior are given by the plot of the maximum crystallization time $t_{\max}$ (on logarithmic scale) versus the crystallization temperature shown in Figure 4. Data points above 255°C were obtained directly from melt crystallization, whereas data points below 255°C were measured from cold crystallization. The plot showed the well-known bell shape as a consequence of the two main competing factors governing the overall rate of crystallization. The first is the nucleation process, which is the controlling factor at high crystallization temperatures and causes $t_{\max}$ to increase with T_c; while the second is the molecular mobility, which dominates at low crystallization temperatures so $t_{\max}$ raises as T_c decreases. We must extrapolate the minimum crystallization peak time from the high- and low-temperature data. It can be noted that the extrapolated maximum peak time is about 0.62 min at 260°C, which is higher than that of PEEK (0.07 min at 230°C).[14] This also implies that the maximum rate of crystallization occurs around 260°C, which

Table I Parameters n, k, t_{max}, t'_{max}, $t_{1/2}$, $\tau_{1/2}$ from Avrami Analysis and Crystallization Enthalpy ΔH_c of Isothermal Melt and Cold Crystallization for PEDEKmK

T_c (°C)	n	k (min^{-n})	t_{max} (min)	t'_{max} (min)	$t_{1/2}$ (min)	$\tau_{1/2}$ (min^{-1})	ΔH_c (J g^{-1})
Cold Crystallization							
245	4.4	0.002	3.87	3.27	3.78	0.26	31.0
246	4.4	0.005	3.14	3.00	3.07	0.33	33.0
247	4.3	0.013	2.58	2.44	2.52	0.40	33.1
248	3.7	0.067	1.91	1.79	1.88	0.53	32.3
250	3.6	0.573	1.07	0.98	1.05	0.95	30.7
Melt Crystallization							
260	2.1	1.50	0.62	0.61	0.69	1.45	38.1
264	2.1	1.26	0.64	0.66	0.75	1.33	37.3
268	2.1	0.82	0.77	0.81	0.92	1.09	42.9
272	2.0	0.51	1.02	0.99	1.16	0.86	43.3
276	2.1	0.24	1.43	1.45	1.66	0.60	42.7

will be displayed on the change of lamellar thickness l_c (presented in Table II).

Activation Energy of Crystallization

The crystallization rate parameter k is assumed to be thermally activated. Then it can be approximately described by an Arrhenius form[11]:

$$k^{1/n} = k_0 \exp(-\Delta E/RT) \qquad (3)$$

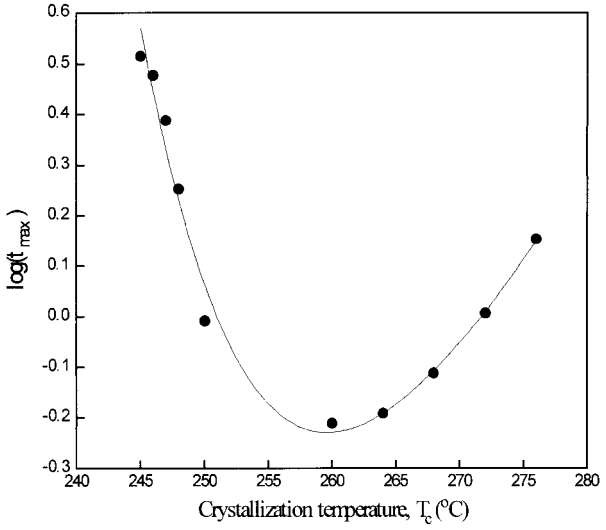

Figure 4 Crystallization peak time t_{max} (on logarithmic scale) versus crystallization temperature T_c for the overall crystallization process.

where k_0 is a temperature-independent preexponential factor and ΔE is a total activation energy which consists of the transport activation energy ΔE^* and the nucleation activation energy ΔF. The slopes of plots of $1/n \ln(k)$ versus $1/T$ determine $\Delta E/R$ (Fig. 5). The values of the activation energy for the primary crystallization process were found to be −118 kJ/mol for crystallization from the melt and 510 kJ/mol for crystallization from the rubbery amorphous state. Since it has to release energy while transforming the molten fluid into the crystalline state, the value of ΔE for the melt crystallization is negative in light of the concept of heat quantity in physical chemistry. On the contrary, as it has to absorb energy while transforming the amorphous glassy state

Table II Lamellar Thickness l_c, Apparent Melting Point T_m, and Enthalpy of Fusion ΔH_m at Different Annealing Temperatures T_a

T_a (°C)	l_c (nm)	T_m (°C)	ΔH_m (J g^{-1})
230	3.20	301.7	41.4
240	3.32	301.8	43.6
250	3.70	302.4	43.8
260	4.48	302.8	44.1
270	4.95	302.9	44.5
280	5.31	303.0	47.4
290	5.77	303.1	47.9

Annealing time: 1 h.

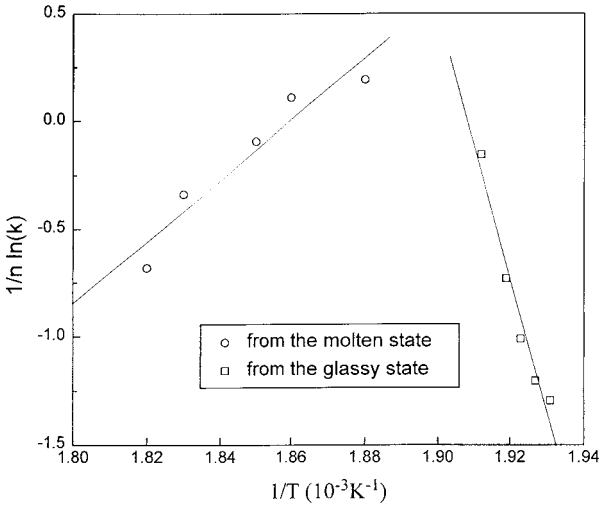

Figure 5 $n^{-1}\ln(k)$ versus T^{-1} for Avrami parameter k deduced from isothermal crystallization data.

into the crystalline state, the value of ΔE for cold crystallization is positive. Moreover, the activation energy of melt crystallization for PEDEKmK was smaller in magnitude than that of crystallization from the glassy state. This result can be explained as follows. The classical concept of crystal nucleation is based on the assumption that fluctuations in the supercooled phase can overcome the nucleation barrier caused by the surface of the crystal. On the one hand, the temperature dependence of the transport activation energy ΔE^* is expected to be similar to the temperature dependence of viscosity. At high temperature (here, for melt crystallization), ΔE^* is almost constant. At low temperature, it increases rapidly as T_g is approached.[13] This can be readily deduced from the Williams–Landel–Ferry equation[15] which was universally used to describe the temperature dependence of polymer melt viscosity. On the other hand, the nucleation rate increases rapidly with decreasing temperature over a relatively narrow temperature interval due to the rapid decrease in the nucleation activation ΔF. At larger degrees of supercooling (here, for cold crystallization), the nucleation rate decreases due to the increase in ΔF when T_g is approached. Accordingly, the maximum level of nucleation rate is critically dependent on the ease with which the crystallizing unit can cross the phase boundary.[13] Since the energy barrier overcome by the supercooled phase for melt crystallization is smaller than that for cold crystallization, the consequence is that the total activation energy ΔE of melt crystallization is smaller than that of cold crystallization, and that the melt crystallization rate $\tau_{1/2}$ is larger than the cold one.

In addition, it is very useful to compare our results of PEDEKmK activation energy to those of PEEK previously reported. The activation energy of PEDEKmK for melt crystallization is remarkably lower than that of PEEK (68 kcal/mol). Yet, the activation energy of cold crystallization is much higher than that of PEEK (52 Kcal/mol).[11] Since ΔE is the activation energy required to transport molecular segments to the crystallization surface, and due to the flexible molecular chain of PEDEKmK linked in the *meta*-form, the value of ΔE in quantity for PEDEKmK is relatively small compared to that of PEEK for melt crystallization. Besides, it is well known that the thermal history in the melt could affect the crystallization behavior of polymer. Thus unmolten crystalline seeds or local chain organization could still remain at temperatures above the melting point.[16] Accordingly, the presence of such primary nuclei decreases the crystallization free energy barrier ΔE and thus increases the crystallization rate. Such a phenomenon is also defined as self-nucleation. Therefore, for cold crystallization heating from the amorphous glassy state, the stiffer and more orderly packed molecular segments of PEEK which can be considered as the local order section may serve as the primary nuclei and can induce the cold crystallization. This would result in a decrease in cold crystallization free energy barrier and an increase in cold crystallization rate, that is to say, the ΔE value of PEEK in magnitude is smaller than that of PEDEKmK for cold crystallization.

Equilibrium Melting Point

Before carrying out the quantitative analysis of the crystallization behavior for polymers the equilibrium melting point temperature (mpt) must be determined as accurately as possible, since the thermodynamic parameters derived from the experimental nucleation parameter K_g are very sensitive to its values. However, the experimental T_ms derived from optical microscopy frequently reflect the melting of the reorganized crystals, not those formed at T_c. Consequently, a careful DSC study should be performed to estimate the equilibrium mpt for polymers. Heretofore, two main well-known approaches have been used to estimate the equilibrium melting point of polymers, i.e., the Hoffman–Weeks and Thomson–Gibbs equations.

According to theoretical consideration by Hoff-

man and Weeks,[17] the equilibrium mpt can be obtained by the intersection of the resulting straight line with the line $T_m = T_c$. Assuming chain folding during crystallization, the dependence of the T_m on the T_c is given by

$$T_m = T_m^0\left(1 - \frac{1}{2\beta}\right) + \frac{1}{2\beta}T_c \qquad (4)$$

where T_m^0 is the equilibrium melting point and β is the lamellar thickening factor which describes the growth of lamellar thickness during crystallization. Under equilibrium conditions, β is equal to 1. At the higher T_c, the slope of the plots was 0.5 and extrapolated to a thermodynamic equilibrium mpt of $T_m^0 = 309$°C for PEDEKmK (Fig. 6). This value is rather lower than those previously reported for PEEK.[14] In the literature, the reported values of T_m^0 for PEEK significantly differed from each other and ranged from 359 to 395°C.[18–23] Such remarkable discrepancies may be attributed to two main factors. First, they are due to the different ways of estimating the equilibrium mpt. Some authors[14,19] employed the fundamental Thomson–Gibbs equation,[20] which considers the depression of melting point that an infinitely thick crystal would suffer when it is divided into lamellar structures whose thickness is l_c. More authors[19,21–23] used another most common method, the Hoffman–Weeks equation, which considers the extrapolation of the experimental melting

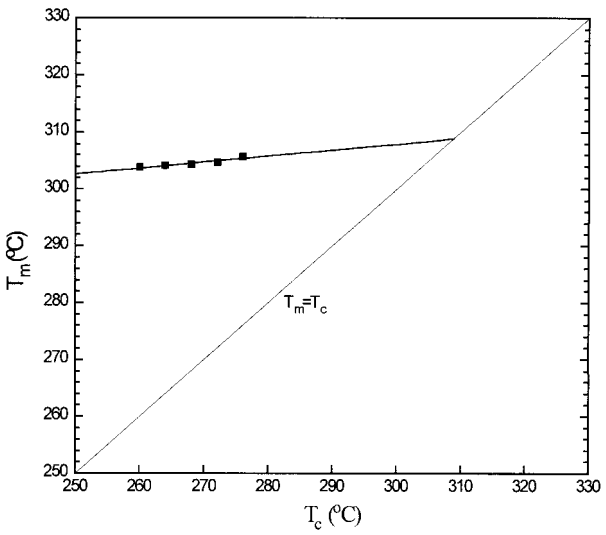

Figure 6 Application of Hoffman–Weeks approach to PEDEKmK for determining its equilibrium melting temperature T_m^0.

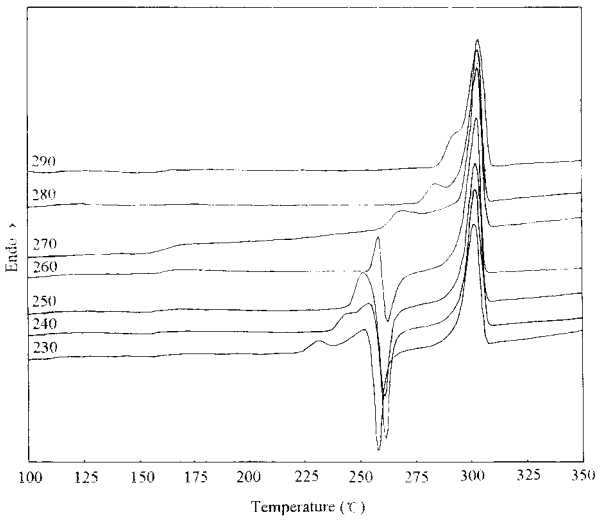

Figure 7 DSC diagrams of PEDEKmK annealed at indicated temperature (T_a) for 1 h. Scanning rate is 20°C/min.

points to a line that represents a crystal that melts at its own crystallization temperature of such crystals. Moreover, the optical microscopic approach is sometimes applied to observe the melting behavior of PEEK. It is owing to these different methods of determinating T_m^0 that several values are often reported for a given polymer. Second, high-temperature polymers [especially poly(aryl ether ketone)s, in general] show multiple melting endotherms, and this often gives rise to controversies with respect to which one is the most appropriate melting point.

Figure 7 shows DSC diagrams of PEDEKmK at different indicated annealing temperatures (T_a). It can be seen that PEDEKmK shows the typical multiple melting endotherms for different T_a. The first/lower melting peak shifts toward the high temperature region with increased annealing temperature. But, the last/higher main melting peak is almost unchanged as T_a increases, which represents the main melting process of the crystals. Accordingly, we consider the melting point at the last endotherm as the point from which extrapolations should be made in order to determine the equilibrium mpt.

In order to verify the value of the foremention ed T_m^0 for PEDEKmK derived by the Hoffman–Weeks method, it is necessary to estimate the equilibrium mpt by using the Thomson–Gibbs approach. When large equilibrium crystals cannot be grown for a direct measurement of the T_m^0, the most precise and best-understood way to estimate T_m^0 is to measure the T_m of well-defined small crys-

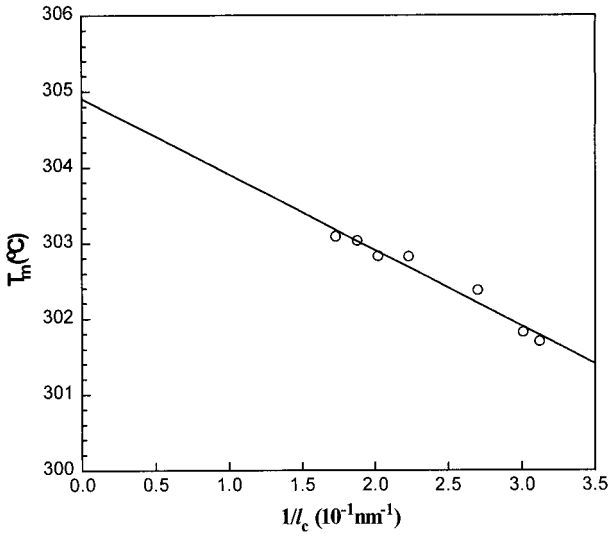

Figure 8 Application of Thomson–Gibbs method to PEDEKmK for estimating its equilibrium melting point T_m^0.

tals, followed by extrapolation to infinite size using the Thomson–Gibbs equation for chain-folded lamellae crystals[24]:

$$T_m = T_m^0\left(1 - \frac{2\sigma_e}{l_c\Delta h_f^0}\right) \tag{5}$$

where σ_e is the end surface energy of planar surface of lamellae, l_c is the lamellar thickness, and Δh_f^0 is the bulk enthalpy of fusion per unit volume for fully crystalline polymer. The values of l_c determined by SAXS and the observed apparent melting point T_m for PEDEKmK annealed at different temperatures are listed in Table II. Figure 8 illustrates a plot of T_m versus $1/l_c$. The points lie on a reasonably straight line which extrapolates for $1/l_c \to 0$ to give an estimate of $T_m^0 = 305$°C. In fact, the values so obtained are near those given by a plot of T_m against T_c, but from which many differ by a few degrees kelvin even for the same samples. Therefore this value is satisfactorily consistent with the one derived from the Hoffman–Weeks equation; and, usually, the values of T_m^0 given by the two approaches tend to be a few K higher than the maximum melting points measured in practice. The T_m^0 value of PEDEKmK is lower than those of PEEK (359°C) and PEEKK (371°C)[25]; the cause of such differences can be reasonably interpreted as the flexibility and stiffness of polymer chains which results from the different linkage forms and various ether/ketone ratios in the polymer chains. At the same time, eq. (5) presents an apparently straightforward method of determining the important parameter σ_e from the slope of a graph of T_m against $1/l_c$,[20] and it gives the value of σ_e = 42.67 erg/cm^2 which compares favorably with determination from other method (seen later). According to the well-known Gibbs function, the equilibrium mpt may be written as

$$T_m^0 = \frac{\Delta H_m^0}{\Delta S_m^0} \tag{6}$$

where ΔH_m^0 and ΔS_m^0 are equilibrium melting enthalpy and entropy, respectively. Therefore, the value of ΔS_m^0 is determined to be 0.40 kJ/(kg °C), which is larger than those of PEEK (0.36 kJ kg^{-1} °C^{-1}) and PEEKK (0.38 kJ kg^{-1} °C^{-1}).[25] Since the entropy is an embodiment of the degree of molecular disorder, this numerical relation is also evident from the composition of repeat unit and the style of linkage for the three polymers.

Spherulitic Growth Analysis

Nucleation Rate Parameter

The spherulitic growth rate G of PEDEKmK was analyzed using the Lauritzen–Hoffman equation[26]:

$$G = G_0\exp\left[-\frac{U^*}{R(T_c - T_\infty)}\right] \times \exp\left[-\frac{K_g}{T_c(\Delta T)f}\right] \tag{7a}$$

where G_0 is a preexponential factor, U^* is the transport activation energy, T_∞ is a hypothetical temperature below which all viscous flow ceases, K_g is a nucleation parameter, ΔT is the degree of supercooling, and f is a correction factor to account for the variation in Δh_f^0 with temperature, $f = 2T_c/(T_m^0 + T_c)$. The "universal" values of U^* = 1500 cal/mol and $T_\infty = T_g - 30$ K were used here in all calculations. It is often most convenient to rearrange eq. (7a) as

$$\log G + \frac{U^*}{2.3R(T_c - T_\infty)} = \log G_o - \frac{K_g}{2.3T_c(\Delta T)f} \tag{7b}$$

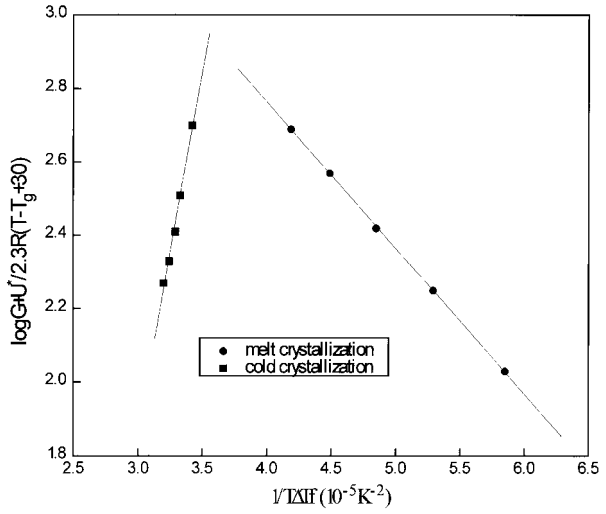

Figure 9 Plots of $[\log + U^*/2.3R(T - T_g + 30)]$ versus $1/(T\Delta T_f)$ for PEDEKmK.

and view the growth rate data in the form of a plot of the left-hand side of eq. (7b) versus $1/T_c(\Delta T)f$, with the slope $= -K_g$ (Fig. 9). Hence, the values of K_g are 9.14×10^4 K^2 and 4.56×10^5 K^2 for isothermal melt and cold crystallization, respectively. Since there are a number of residual nuclei seeds in the amorphous glassy state, it is easily understood for the quantitative relation of $K_{g,\text{melt}} < K_{g,\text{cold}}$.

Lauritzen Z-test

It is well known that the nucleation constant K_g takes the form[26]

$$K_g = \frac{nb_0\sigma\sigma_e T_m^0}{\Delta h_f^0 k} \qquad (8)$$

where b_0 is the thickness of a monomolecular layer, σ is the lateral surface free energy, k is the Boltzmann constant, and n takes on a value of 4 in regime I or III and a value of 2 in regime II. In order to investigate to which regime the data in the selected temperature region (i.e., from 245 to 276°C) belong, we employed the Lauritzen Z-test.[27] Z is defined as

$$Z \cong 10^3(L/2a_0)^2\exp[-X/T_c(\Delta T)] \qquad (9)$$

where L is the effective lamellar thickness and a_0 is the chain stem width. Regime I kinetics are followed if substitution of $X = K_g$ into eq. (9) results in $Z \leq 0.01$. If $X = 2K_g$ is substituted and eq. (9) yields $Z \geq 1$, then regime II kinetics are followed. Since we do not yet know which crystallographic plane represents the preferred growth face, we have followed the dictates of the Bavais–Friedel law, which states that the preferred face will be the crystal plane with the largest spacing. Therefore, according to the lattice parameters of PEDEKmK given in our previous paper,[7] this preferred growth plane will be (110), which will give a growth step (i.e., the thickness of a monomolecular layer) of $b_0 = 0.494$ nm and the width of the molecular chain $a_0 = 0.477$ nm. Moreover, from Table II, one can find that the thickness of lamellae l_c vary from 3.20 to 5.77 nm in the crystallization temperature region of 230 to 290°C. With all the above-mentioned results, the regime of crystallization is easily determined to be regime II, i.e., numerous surface nuclei involved in formation of substrate, thereby $K_g = 2b_0\sigma\sigma_e T_m^0/\Delta h_f^0 k$.

Surface Free Energy (σ, σ_e) and Work of Chain Folding (q)

The derived K_gs can be used to calculate the end surface free energy σ_e and the work of chain folding q for PEDEKmK from eq. (8) (where $n = 2$). Using the value of $T_m^0 = 309$°C and $\Delta h_f^0 = 125$ J/g,[5] the $\sigma\sigma_e$ products were derived. The primary difficulty in estimating q (via σ_e) is that of determining the lateral surface free energy, σ. The usual approach is to estimate σ from the Thomas–Stavely relationship[26]:

$$\sigma = \alpha\Delta h_f^0(a_0b_0)^{1/2} = \alpha\Delta h_f^0 A_0^{1/2} \qquad (10)$$

where A_0 is the cross-sectional area of a chain in the crystal, and α is an empirical constant which usually ranges between 0.1 and 0.3. In common, $\alpha = 0.1$ for hydrocarbons, e.g., polyolefins; $\alpha = 0.24$ for polyesters, e.g., poly(pivalolactone) and poly(phenylene sulfide)[28]; and $\alpha = 0.3$ for most organics.[18] At this juncture, however, it is not possible to predict the appropriate α, given a chemical structure. Therefore, the tack we took was to calculate σ, σ_e, and q using these three values, assessing which (if any) produces clearly more reasonable values. The values of q calculated with $\alpha = 0.24$ (or 0.25) and $\alpha = 0.3$ are unrealistically small (there, q is about 1.1–1.4 kcal/mol); therefore, we shall discuss only values derived with $\alpha = 0.1$. Thus, σ was estimated to be 8.45 erg/cm^2; and, from the $(\sigma\sigma_e)$ product, σ_e was determined as 45.17 erg/cm^2, which is well compatible with the result derived from eq. (5).

The work of chain folding per molecular fold can be obtained as[29]

$$\sigma_e = \sigma_{e0} + q/(2A_0) \approx \sigma + q/(2A_0) \quad (11a)$$

where σ_{e0} is the value that σ_e would assume if no work were required to form the fold; and q is the work required to bend a polymer chain back upon itself, taking into account the conformational constraints imposed on the fold by the crystal structure. As a first approximation, σ_{e0} may be taken as roughly equal to the lateral surface energy, σ. It is expected, therefore, that σ_{e0} will be significantly less than $q/(2A_0)$ and, consequently, may be set equal to zero as the second approximation. Accordingly, eq. (11a) is usually written as follows:

$$q = 2A_0\sigma_e = 2a_0b_0\sigma_e \quad (11b)$$

For any single polymer, then, σ_e was considered to be inversely proportional to the chain area, the proportionality constant being $q/2$. This leads to values for the work of folding of 2.13×10^{-20} J per molecular chain fold, i.e., 3.06 kcal/mol for PEDEKmK.

The work of chain folding q has been found to be the one parameter most closely correlated with molecular structure, and probably the most important contribution to its relative magnitude is thought to be the inherent stiffness of the chain itself.[26] For example, polymers with flexible chains, such as polyethers, have q values near 3–4 kcal/mol[26,30]; intermediate ones (e.g., PEEK and PEEKK, with q's of 4.11 and 4.25 kcal/mol, respectively[25]) have q values close to 4–5 Kcal/mol; and stiffer ones [e.g., isotactic polystyrene and poly(phenylene sulfide)] have qs in the range of 7–9 kcal/mol.[26,28] The calculated work of chain folding for PEDEKmK corresponding to σ_e = 45.17 erg/cm^2 is surpringly small—on the order of 3 to 4 kcal/mol. This is obviously associated with the incorporation of *meta*-phenyls in the crystal which makes it easy to form a chain folding while crystallizing. The thermodynamic and kinetic data of several poly(aryl ether ketone)s are collected in Table III, illustrating that these parameters systematically and reasonably change with the variation in rigidity of polymer molecular chains.

Table III Collection of the Thermodynamic and Kinetic Parameters for Different Poly(aryl ether ketone)s

PAEKs	PEDEKmK	PEEK	PEEKK
T_g (°C)	160	144	149
$T_{c,h}$ (°C)	265	176	181
$T_{c,c}$ (°C)	251	290	302
T_m (°C)	303	335	362
T_m^0 (°C)	309	359	371
ΔH_m^0 (J g^{-1})	125	130	140
ΔS_m^0 (J g^{-1} °C^{-1})	0.40	0.36	0.38
σ (erg cm^{-2})	8.45	8.72	9.53
σ_e (erg cm^{-2})	45.17	59.89	59.63
q (kcal mol^{-1})	3.06	3.96	3.98

All DSC scanning rates are 10°C/min.

CONCLUSIONS

A systematic study of the isothermal melt and cold crystallization kinetics of PEDEKmK was performed by DSC over two crystallization temperature regions. The typical Avrami plots indicate that the Avrami analysis can gratifyingly describe the primary stage of both crystallization processes, and the deviation of linearity at the "tails" of lines may be ascribed to the occurrence of the spherulite impingement in the secondary stage. For melt crystallization, $n = 2$, it corresponds to a two-dimensional, circular, diffusion-controlled crystal growth, depending on the amount of thermal nucleation. However, for spherulites nucleated sporadically in time growing in three dimensions and having interface control, the Avrami exponent n should be 4 for cold crystallization.

The total activation energy of melt crystallization is determined, which is smaller than that of cold crystallization, and can be explained by the dependence of activation energy on temperature. The consequence is that the melt crystallization rate is higher than the cold one.

The equilibrium mpt T_m^0 derived from two classical approaches (i.e., the Hoffman–Weeks and Thomson–Gibbs equations) are favorably compatible with each other, and their values are a few K higher than the maximum melting points (T_m) measured in practice. Due to the *meta*-linked fashion, T_m^0 of PEDEKmK is remarkably lower than those of PEEK and PEEKK.

From the spherulitic growth equation proposed by Hoffman and Lauritzen, the nucleation parameters K_g of the isothermal melt and cold crystallization were estimated, from which the lateral and end surface free energy (σ and σ_e) and the work of chain folding q were derived. The resultant data were compared with those of the other members

of poly(aryletherketone)s, such as PEEK and PEEKK. The differences between them were interpreted in the terms of the composition of polymer chains (i.e., the ratios of ether/ketone) and the linkage form (i.e., *para*- or *meta*-incorporation style).

REFERENCES

1. P. A. Staniland, *Bull. Soc. Chim. Belg.,* **98,** 667 (1989).
2. I. Y. Chang, *SAMPE Q.,* **19,** 29 (1988).
3. D. J. Blundell, *Polymer,* **33,** 3773 (1992).
4. J. J. Liggat and P. A. Staniland, *Polym. Commun.,* **32,** 450 (1991).
5. D. J. Blundell, J. J. Liggat, and A. Flory, *Polymer,* **33,** 2475 (1992).
6. S. E. Wang, J. Z. Wang, H. F. Zhang, Z. W. Wu, and Z. S. Mo, *Makromol. Chem. Phys.,* to appear.
7. S. E. Wang, J. Z. Wang, Z. S. Mo, H. F. Zhang, and Z. W. Wu, *Makromol. Chem. Phys.,* to appear.
8. O. Glatter, *J. Appl. Crystallogr.,* **10,** 415 (1977).
9. M. Avrami, *J. Chem. Phys.,* **7,** 1103 (1939).
10. M. Avrami, *J. Chem. Phys.,* **8,** 212 (1940).
11. P. Cebe and S.-D. Hong, *Polymer,* **27,** 1183 (1986).
12. Y. Lee and R. S. Porter, *Macromolecules,* **21,** 2770 (1988).
13. B. Wunderlich, *Macromolecular Physics,* Vol. 2, Academic Press, New York, 1977.
14. D. J. Blundell and B. N. Osborn, *Polymer,* **24,** 953 (1983).
15. M. L. Williams, R. F. Landel, and J. D. Ferry, *J. Am. Chem. Soc.,* **77,** 3701 (1955).
16. Y. Lee and R. S. Porter, *Macromolecules,* **21,** 2770 (1988).
17. J. D. Hoffman and J. J. Weeks, *J. Chem. Phys.,* **37,** 1723 (1962).
18. F. J. Medellin-Rodriguez, P. J. Philips, and J. S. Lin, *Macromolecules,* **28,** 7744 (1995).
19. H.-L. Chen and R. S. Porter, *J. Polym. Sci., Part B., Polym. Phys. Ed.,* **31,** 1845 (1993).
20. D. C. Bassett, *Principles of Polymer Morphology,* Cambridge University Press, Cambridge, 1981.
21. G. C. Alfonso, V. Chiappa, J. Liu, and E. R. Sadiku, *Eur. Polym. J.,* **27,** 795 (1991).
22. J. N. Hay and D. J. Kemmish, *Plast. Rub. Proc. Appl.,* **11,** 29 (1989).
23. Y. Lee and R. S. Porter, *Macromolecules,* **20,** 1336 (1987).
24. B. Wunderlich, *Macromolecular Physics—Crystal Melting,* Vol. 3, Academic Press, New York, 1980.
25. T. X. Liu, Z. S. Mo, S. E. Wang, H. F. Zhang, H. Na, and Z. W. Wu, unpublished data.
26. J. D. Hoffman, G. T. Davis, and J. I. Lauritzen, *Treatise on Solid State Chemistry,* Vol. 3, H. B. Hannay, Ed., Plenum, New York, 1975.
27. J. I. Lauritzen, *J. Appl. Phys.,* **44,** 4353 (1973).
28. A. J. Lovinger, D. D. Davis, and F. J. Padden, *Polymer,* **26,** 1595 (1985).
29. J. I. Lauritzen and J. D. Hoffman, *J. Res. Natl. Bur. Stds.,* **64A,** 73 (1960).
30. J. Runt, R. F. Wagner, and M. Zimmer, *Macromolecules,* **20,** 2531 (1987).